

Fractal nature of electrical conductivity in ion-implanted polymers

B. Wasserman*

Massachusetts Institute of Technology, Department of Physics, Cambridge, Massachusetts 02139

(Received 9 January 1986)

The electrical-conductivity and current-transient data for ion-implanted polymers are explained in terms of a percolative phase transition from an insulating state to trap-controlled hopping conduction on a backbone cluster. The value of the critical exponent s' for electrical conductivity versus the fluence ranges from ~ 4 to 5, consistent with the fractal behavior in the vicinity of the phase transition. The percolative stabilization of radicals is suggested as a reason for the sharp increase in the unpaired spin concentration within the damage structures, recorded by the ESR measurements. A scaling relation between the free spin concentration and ESR linewidth, including an exponent d_{\min} [$\sim 1.2 \pm 0.05$ for poly(2,6-dimethylphenylene oxide)] is established. The change in s' , as a function of ion energy, is connected with the crossover between nuclear and electronic energy transfer. The one-dimensional character of the temperature dependence of the electrical conductivity is related to the links connecting the groups of traps. The contribution of dangling bonds is suggested as a reason for the lagging of the percolation threshold in the conductivity measurements, as compared to ESR. The fractal exponent α of the dielectric relaxation is measured versus fluence from the current transients (α between 0.22 and 0.85). A sharp increase in the real part of the dielectric constant at low frequencies is observed, as expected for fractals.

I. INTRODUCTION

Fractal concepts play an increasingly important role in the interpretation of phenomena occurring on grain boundaries, in porous media, and in embedded and ballistically generated aggregates. There is special interest in fractal concepts for polymeric compounds. For example, fractal hopping time distributions were studied for naphthalene-doped polymeric glass powders and films (polymethylmethacrylate, polystyrene), etc.¹

As was reported previously² the process of ion implantation in a variety of polymeric compounds leads to a tremendous enhancement in the electrical conductivity,^{2,3} in the ESR signal of free radicals,⁴ as well as in the optical absorption⁵ and in current transients.⁶ Various models were proposed to explain this unusual phenomenon as, for example, the charged-grain model³ and Mott's variable-range hopping conduction.² In this paper the author suggests that ion-implanted polymers provide a novel system for performing comprehensive experimental studies on fractals.

The discussion presented here is based on a set of experimental results using a variety of techniques and is intended to elaborate the mechanism of the electrical conductivity and spin diffusion in ion-implanted polymers by using a fractal formalism. An extension of fractal concepts to polymer statistics can be found in the review article of Stanley.⁷ Fractal dimensions for the percolation cluster, consisting of "links" connecting the "blobs," are introduced in that paper. Here, we shall try to apply these definitions to a number of phenomena recently observed in ion-implanted polymers.

II. EXPERIMENTAL BACKGROUND

The technique that was utilized for thin-film deposition was the spin-casting method. For this method, a glass-

slide substrate, shaped in a 1×1 -in.² square, was attached to a spinner chuck. The rotation speed could be varied up to 2500 rpm. A drop of solution was deposited on the substrate by using either a dropper or a Manostat syringe with a $0.2\text{-}\mu\text{m}$ micropore filter to obtain high-purity films.

The solvent chloroform was used to prepare the poly(2,6-dimethylphenylene oxide) (PPO) film. Polyacrylonitrile (PAN) was deposited from a saturated solution using the solvent *N,N*-dimethylformamide, at a temperature between 120 and 140°C. Thin films with thicknesses in the range 0.5 to 1 μm were prepared, as measured by a Dektak profilometer. The preparation of poly(4-phenyl-2,6-quinoline) (PQ) and the results of ion implantation on the properties of PQ are described in the work of Wnek *et al.*⁸

All the polymer samples in this work were implanted at 200 keV to various fluences using an Accelerators Incorporated model No. 300 MP ion implanter. To prevent excessive heating of the polymer the beam currents did not exceed $\sim 10\ \mu\text{A}$. At beam currents of $10\ \mu\text{A}$ the temperature rise of the sample surface was estimated to be $\sim 125^\circ\text{C}$. The techniques, used for the measurements of the electrical conductivity, the unpaired-spin concentration, and the ESR linewidth are described elsewhere.^{2,4} The residual gas analysis was performed *in situ* by attaching a Veeco Instruments SPI-10 residual gas analyzer to the port of the ion implanter.

The metal-oxide-semiconductor (MOS) capacitor configuration, designed and calculated by Khan and Adler⁹ was chosen for our measurements of current transients. In this configuration the drain and the source are short-circuited and a 5000-Å-thick SiO_2 layer was thermally grown on the surface of a highly conductive Si wafer, used as a gate. Polymer films were spin cast on the SiO_2 surface from the carefully filtered solution and implanted

at 77 K to prevent pyrolysis. Cr drain-source electrodes were evaporated on the top of the sample through a mask machined in a transmission-line configuration. Current transients were taken with the help of a Textronics oscilloscope (7D20 programmable digitizer). The log-log current versus time dependences were analyzed with the help of a MINC 11/23 computer.

III. DISCUSSION

As was mentioned in our previous reports,^{2,3} ion implantation causes an increase, by ~ 14 orders of magnitude, in the electrical conductivity of normally insulating polymers such as polyacrylonitrile, poly(2,6-dimethyl-phenylene oxide), and poly(4-phenyl-2,6-quinoline) after ion implantation with Br, As, Kr, and N at energies greater than 200 keV and fluences greater than 3×10^{15} ions/cm². For these implantations we have found no correlation of the conductivity increase with the ion species.

According to the Lindhard-Scharff-Schiott (LSS) theory,¹⁰ a single ion impinging on the polymer sample with 200 keV has a penetration depth $R_p \sim 2500$ Å and straggling ranges $\Delta R_{p\perp} \sim 120$ Å and $\Delta R_{p\parallel} \sim 350$ Å (see Fig. 1). As shown by our calculations, the ion-induced damage in this energy range is determined by the nuclear stopping power. The maximum number of defects per unit area N , created by implantation is defined in the LSS theory by $N \sim N_a(dE/dx)/E$, where N_a is the fluence, dE/dx is the energy transfer per unit depth, and E corresponds to the ion energy.

Some of the atoms in the damaged region will be completely removed from their original positions, and some will be slightly displaced during this single-collision event. The probability of the displacement is proportional to the energy of the ion E and the average molecular weight of the polymer, and depends on the elastic properties of the material. A significant amount of strain is introduced in the molecular lattice. The overall geometry of the damaged region resembles the well-studied "tree" structure, incorporated in a blob (see Fig. 1).

Dense clustering of the damaged blobs is expected to occur at fluences $\sim 10^{14}$ ions/cm², just below the observed sharp increase in the ESR spin concentration. However, taking into account the radical-vacancy recombination process at the early stage of implantation, the real sizes of blobs with the nonrecombined free radicals are expected to be significantly smaller than those calculated from the LSS theory.

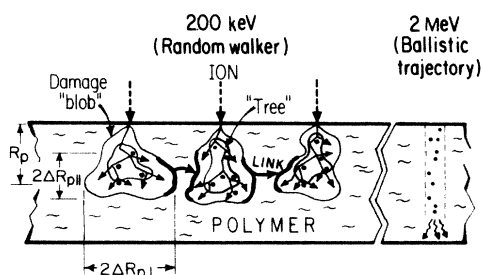


FIG. 1. Schematic diagram of the ion-damaged region.

A. Free-radical formation

At low fluences ϕ from about 10^{11} to 10^{13} ions/cm², two competing processes take place. The completely displaced ions and those with all damaged bonds start to form localized states, with free radicals and vacancies. Partially displaced ions with free radicals have a high probability of recombination with vacancies, forming neutral dimers, trimers, and fused rings. In fact, ion-induced polymerization was experimentally observed by Elman *et al.*,¹¹ by taking the Raman spectra of the implanted diacetylene. At this stage, the amount of free hydrogen present close to the damaged area is greater than the number of nonrecombined free radicals created via ion implantation. Thus, the implantation process is followed by a subsequent recombination with hydrogen, giving almost no rise in the ESR signal. After a vast amount of hydrogen has left the polymer sample, in accordance with the peak in the hydrogen evolution, recorded by the *in situ* residual gas analysis^{5,12} [see Fig. 2(a)] and the large reduction in the sample thickness (by 2500 Å), the number of free radicals is expected to increase with fluence [see the curve crossing in Fig. 2(a)]. The correlation between the H₂ evolution and the onset of free-radical formation is, thus, straightforward.

At the point where the number of free radicals, created by ion implantation, approaches a maximum, any further

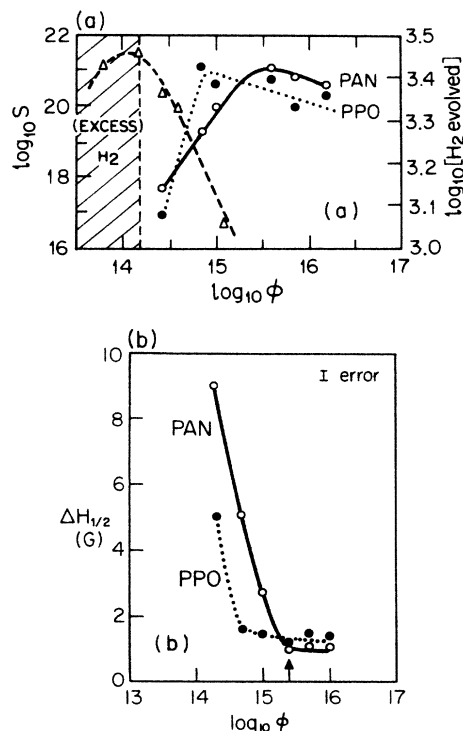


FIG. 2. (a) Free spin concentration versus ⁸⁴Kr ion fluence for PAN (solid line) and PPO (dotted line) samples implanted at 200 keV. The dashed line corresponds to the amount of evolved hydrogen [H₂ evolved]. (b) ESR linewidth (half width at half maximum) dependence on fluence for ⁸⁴Kr implanted into PAN (solid curve) and PPO (dotted line) at 200 keV.

increase in fluence just causes damage via induced recombination. A slight decrease in the ESR signal with fluence is observed around the value 3×10^{15} ions/cm² as a result [see Fig. 2(a)].

The suggested mechanism for the critical enhancement of the concentration of free spins is the percolative stabilization of radicals above a certain fluence. The total cluster mass of the radical blobs N_F , each including an ion trace tree (see Fig. 1), scales as

$$N_F \sim \xi^{d_l} \sim (p - p_c)^{-\nu d_l}, \quad (1)$$

following the arguments of Ref. 7, where d_l is the chemical or "spreading" dimension, measuring the number of trees of defects created via collisions during ion implantation (see Fig. 1), where ξ is the pair-connectedness length, ν is the critical exponent for the pair-connectedness length ($\nu = \frac{1}{2}$ in the classical theory), p is the probability of site occupation by a free radical, and p_c is the critical percolation probability. We introduce a critical exponent x , reflecting the connection between the blob-size distribution function and the implantation fluence via

$$p - p_c \sim (\phi - \phi_c)^x. \quad (2)$$

Then

$$N_F \sim (\phi - \phi_c)^{-x\nu d_l}. \quad (3)$$

Since the recombination rate of free radicals is determined by the radius of localization or blob size, the sharp onset of the ESR signal at a fluence of $\sim 3 \times 10^{14}$ cm⁻² follows immediately. We also observed a sharp decrease in the ESR linewidth, indicating the delocalization of radicals within a blob, with subsequent saturation. A strong decrease of the spin-carrier scattering time $\tau \sim \Delta H_{1/2}^{-1}$ (full width at half maximum) above a critical fluence ϕ_c can be deduced from the Fig. 2(b).

From the values of scattering time one can estimate the "chemical length" for a spin carrier between spin flips within a blob $l \sim v_F \tau_{\text{spin}}$. The velocity v_F is calculated from $v_F \sim N_F^{1/d_l} \hbar/m$ by inserting the spin concentration at corresponding fluences [see Fig. 2(a)]. The spin-flip time estimate for these fluences were taken from our early analysis of the ESR line shape in the wings.⁴ The correlation ("air") distance ξ between two points is estimated from the spin concentrations at these fluences by $\xi \sim N_F^{-1/d_l}$. After evaluation of

$$l \sim \xi^{d_{\min}}, \quad (4)$$

we obtain $d_{\min} \approx 1.2 \pm 0.05$ for PPO, by taking $d_l = 2$ for branched polymers.¹³ The scaling dependence establishes an explicit relation between the spin concentration and linewidth in implanted polymers.

B. Electrical conductivity

Although ion implantation is assumed to provide macroscopically uniform damage, the microscopic chain clustering, present in the pristine polymer, leads to a clustering, or grouping of the ion-damaged regions. The dc conductivity can be calculated in terms of the inter-

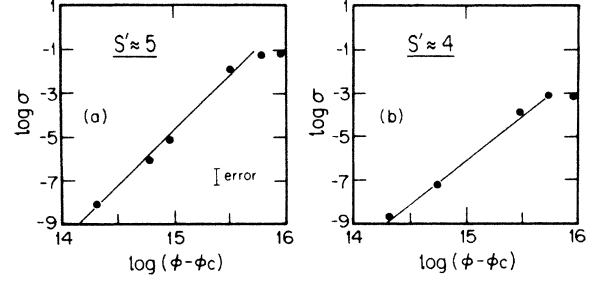


FIG. 3. Theoretical fit for fluence dependence of conductivity (a) for PAN, (b) for PPO, implanted at 200 keV (⁸⁴Kr) ($\phi_c = 1 \times 10^{14}$ cm⁻²).

"group" transition probabilities. Each microscopic damage blob in this picture is identified with a site on a hopping lattice with a high local concentration of free radicals ($\sim 10^{22}$ cm⁻³). The effect of the intrablob transitions refers solely to the high-frequency limit of the conductivity, since their transition rates are much faster than the interblob transition rates. Therefore, the damage blob can be considered as a "superconducting" entity. We associate this mechanism with the trap-controlled hopping of the de Gennes termite, since the hopping rates are modulated by the capture and release rates of the traps. In a real situation, the linking of the superconducting blobs is obtained via the implantation-induced polymer crosslinking (see Fig. 1).

According to Stanley,⁷ the self-avoiding random-walk problem for a termite leads to a scaling estimate of the electrical conductivity σ

$$\sigma \sim \xi^{\tilde{s}} \sim \xi^{d_f - d_w} \sim (\phi - \phi_c)^{-s'}, \quad (5)$$

where ϕ is the fluence, ϕ_c is the critical fluence, \tilde{s} stands for critical exponent of the conductivity, and ξ is the pair-connectedness length. We have used the notations d_f for the backbone fractal exponent, d_w for the fractal di-

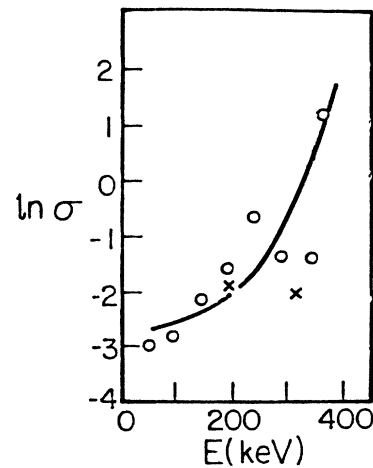


FIG. 4. Implantation energy dependence of conductivity for PAN implanted with ⁸⁴Kr at 1.2×10^{16} cm⁻² for a range of ion energies.

mension of the random walk of a charge carrier within a blob ($d_w \geq 2$), and $s' = x\nu\bar{s}$ is the fractal exponent of the conductivity versus ion fluence. Since our conductive layer is expected to be essentially planar (~ 350 Å), two spatial dimensions ($r_{lm}, \Delta E_{lm}$) and one dimension for the energy were considered for the probability of variable-range hopping $P_{\text{hop}} = P(r_{lm}, \Delta E_{lm})$. The fit to the experimental data gives the critical exponent value $s' \sim 5$ for PAN and $\sim 4(\pm 0.1)$ for PPO (see Fig. 3). The mean-field approach leads us to the analogy with the Bethe tree approximation for gels and for the vulcanization of rubber. The observed insolubility of the implanted polymer is, possibly, related to the crosslinking between the damage blobs, and the model of vulcanization thus seems quite appropriate.

The proposed mechanism explains the lagging of the percolation threshold for the conductivity, compared to the sharp onset of the free radical creation. The dangling bonds contributing to the ESR signal *do not* contribute to the conductivity.

On the basis of the proposed model one can attempt to explain the observed increase of the conductivity (versus energy) at ~ 350 keV (see Fig. 4). The crossover between the nuclear and electronic energy transfer is located at ~ 400 keV, as follows from our calculations for PAN and PPO.⁵ This change of mechanism leads to the replacement of a random walker (RW) (nuclear process) by the ballistic (linear) trajectory (electronic process), as indicated in Fig. 1. The surface size exponents $\gamma = 1/d_f$, characterizing blobs, are different for the two processes, as calculated by Meakin *et al.*¹⁴ ($\gamma_{\text{RW}} = 0.52$, $\gamma_{\text{ball}} = 0.68$). A dramatic increase in s' is observed for the implantation with 2-MeV Ar⁺ ions into the HPR-204 polymer and organic compound PTCDA,^{3,15} as compared to our data for 200 keV (see Table I).

The temperature dependence of the conductivity for fluences in the region of 3×10^{15} cm⁻², as observed by the present author, seems to obey *the variable-range hopping law for one dimension*, being dominated by single links, joining the blobs² (see Fig. 1), with

$$\sigma \sim \sigma_0 \exp(-T_0/T)^{1/2}, \quad (6)$$

where $T_0 = 4a/k_B N(E_F)$ and $N(E_F)$ is the density of states at the Fermi level, a is the coefficient of exponential decay of the localized states, and k_B is Boltzmann's

TABLE I. Comparison of the critical exponents for conductivity in the case of the electronic and nuclear energy transfer.

Polymer or organic film	Energy	Experimental exponent s' (± 0.05)	Energy transfer
PAN	200 keV	5	nuclear
PPO	200 keV	4	nuclear
PQ	200 keV	~ 4.8	nuclear
HPR-204	2 MeV	~ 7	electronic ^a
PTCDA	2 MeV	~ 7	electronic ^b

^aT. Venkatesan, S. R. Forrest, M. L. Kaplan, C. A. Murray, P. K. Schmidt, and B. J. Wilkens, *J. Appl. Phys.* **54**, 3150 (1983).

^bA. J. Lovinger, S. R. Forrest, M. L. Kaplan, P. H. Schmidt, and T. Venkatesan, *J. Appl. Phys.* **55**, 476 (1984).

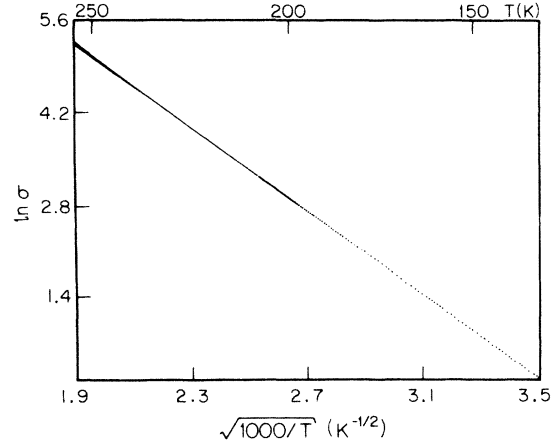


FIG. 5. Temperature dependence of the conductivity of PAN implanted with ⁸⁰Br at $\phi = 2 \times 10^{16}$ cm⁻² and $E = 200$ keV (see text).

constant. The hopping process is governed by the interaction of electrons with phonons of a fractal network. The temperature dependence of the dc conductivity was measured over a wide temperature range ($4.2 < T < 370$ K) for ion-implanted PAN, PPS, PPO, and PQ. A similar T dependence of $\ln(\sigma/\sigma_0) = -(T_0/T)^{1/2}$ was obtained for almost all of the amorphous polymer hosts, implants, fluences, and energies used in this work. Typical experimental results are shown as points in Fig. 5 for ⁸⁰Br ions implanted into PAN at 200 keV and $\phi = 2 \times 10^{16}$ cm⁻² for $80 < T < 280$ K. Though the absolute values of T_0 are highly sensitive to ϕ , the functional form does not change with fluence. It is generally found that T_0 decreases with increasing fluence ϕ . We note, however, that the observed temperature dependence, as well as the detected nonlinearity of conductivity with the sample length, cannot serve as a definitive proof for the dimensionality of our system.

The physical origin of the probability p [see Eq. (3)] is related to the probability that the ion-damage site is occupied by a stable nonrecombined free radical in Eq. (1). The meaning of this quantity in Eq. (5) for the conductivity is the probability for the link to join the corresponding damage blobs. The scaling relation [Eq. (1)] is thus interpreted for the ESR signal of the free-radical number within a single blob, in contrast to the relation in Eq. (5) which gives a scaling relation for the conductivity between linked blobs.

C. Transient current responses

According to Schlesinger and Montroll¹⁶ the dipole relaxation, due to local conformational abnormalities in polymers is governed by the Williams-Watt fractional exponential

$$\varphi_\alpha(t) = \exp[-(t/\tau)^\alpha], \quad 0 < \alpha < 1, \quad (7)$$

where τ is the time constant. Dangling bonds, vacancies, and blob boundaries created via the process of ion implantation introduce local strains in the system. We have studied the current transients in implanted polymers using

the MOS capacitor configuration, described elsewhere.^{5,6,9} The expected time dependence of the current, following from Eq. (7) is

$$I \sim t^{(\alpha/2)-1} \quad (8)$$

This expression is identical with the short-time approximation of the calculated transient current response of our circuit.

By analyzing the experimental results, we observe the *percolative transition* via a sudden increase (by about three orders of magnitude) in the intensity of the current transient⁶ at a fluence of about $1 \times 10^{15} \text{ cm}^{-2}$ (see Fig. 6). The value of the time fractal exponent α obtained from the fit to Eq. (8) in this range of fluences increases from ~ 0.22 to ~ 0.86 , indicating the formation of a conductive cluster. The concept of fractal time thus can be applied here.

Finally, we have observed the anomalous increase in the real part of the dielectric constant κ' at low frequencies, consistent with a $\kappa' \sim \omega^{-y}$ type of behavior, expected for fractals ($1 < y < 2$). The ac conductivity shows an anomalous power law at high frequencies (see Fig. 7).

At the same time the further increase in fluence leads to a strong overlap between the blobs, implying restrictions on the trap-controlled hopping. Since the system becomes homogeneous (Euclidean) on a very fine scale, a slight decrease of the conductivity is observed as a result of the blob-blob interpenetration.

Taking into account the proposed mechanism one

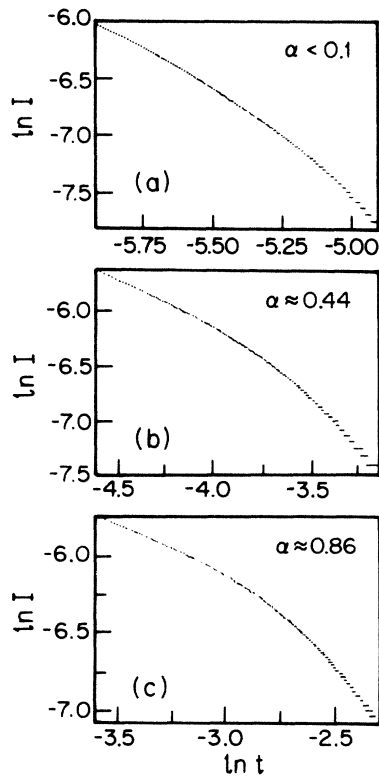


FIG. 6. Current transients for PPO implanted with 200-keV ^{84}Kr ions at fluences (a) $5 \times 10^{14} \text{ cm}^{-2}$, (b) $9 \times 10^{14} \text{ cm}^{-2}$, and (c) $3 \times 10^{15} \text{ cm}^{-2}$.

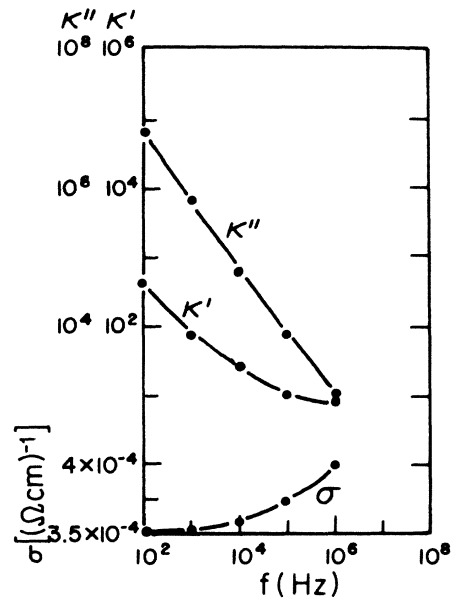


FIG. 7. Frequency dependences of the real and imaginary parts κ' and κ'' of the dielectric constant and of the ac conductivity for the PPO sample implanted with ^{84}Kr at energy 200 keV and at fluence of $3 \times 10^{15} \text{ cm}^{-2}$.

should expect a critical behavior of the elastic properties of the polymer in the investigated fluence range. The preliminary data of Carlson *et al.*¹⁷ for carbon and oxygen ion implantation in a carbon-black-filled poly(1-hexene) elastomer are indicative of a strong abrupt change in elastic modulus at the fluence $\sim 10^{14} \text{ cm}^{-2}$ and energy 6 MeV. The fractal dimension d_e of the elastic backbone can be obtained from these measurements.

By varying the energy loss per unit length dE/dx , via the change in ion energy, it is expected that the value of the critical fluence can sensitively vary along the critical energy-fluence phase diagram $\phi_c E_c = \text{const}$. The experiments for testing this concept are in progress.

IV. CONCLUSIONS

At the early stages of ion implantation (low-fluence range) the rate of radical creation is in stable dynamical equilibrium with the radical-vacancy recombination process. The low-fluence regime $\sim 3 \times 10^{14} \text{ cm}^{-2}$ exhibits a maximum of hydrogen evolution, accompanied by a sharp increase in the number of free radicals. This fact is attributed to the percolative delocalization of free radicals within a blob of a certain size. A scaling relation, including an exponent d_{min} ($\sim 1.2 \pm 0.05$), between the free spin concentration and the ESR linewidth is established.

The intermediate-fluence range (around $3 \times 10^{15} \text{ cm}^{-2}$) is characterized by a sharp percolative transition from the insulating state to a trap-controlled hopping mechanism, as follows from the abrupt change in current transient. The critical exponent for the conductivity versus fluence s' ranges from ~ 4 to 5 for the different polymers implanted at 200 keV, and increases with the implantation energy. The increase is attributed to a crossover between

electronic and nuclear-energy-transfer processes. The conductivity is determined by links between the groups of traps, possibly responsible for the one-dimensional character of the temperature dependence.

The change in the fractal time exponent α (from 0.22 to 0.86) with implantation fluence was determined from the current transients. An anomalous behavior in the real part of the dielectric constant is observed at low frequencies. With further increase in the fluence, the system becomes homogeneous (nonfractal), causing the conductivity to level off or even decrease.

ACKNOWLEDGMENTS

The author is indebted to Professor M. S. Dresselhaus (Massachusetts Institute of Technology), Professor H. E. Stanley (Boston University), Dr. M. Rubinstein (Eastman Kodak), and Professor G. E. Wnek (Massachusetts Institute of Technology) for helpful discussions. Financial support from National Science Foundation, Materials Research Laboratories Program Grant No. DMR-84-18718 is gratefully acknowledged.

*Present address: Max-Planck-Institut für Festkörperforschung, Stuttgart-7000, Federal Republic of Germany.

- ¹R. Kopelman, L. A. Harmon, E. I. Newhouse, S. J. Parus and J. Prasad, MRS Symposium on Fractal Aspects of Materials, Boston, 1985 (unpublished).
- ²B. Wasserman, G. Braunstein, M. S. Dresselhaus, and G. E. Wnek, in *MRS Symposium on Ion Implantation and Ion Beam Processing of Materials*, edited by G. K. Hubler, O. W. Holland, C. R. Clayton, and C. W. White (North-Holland, New York, 1984), Vol. 27, p. 413.
- ³T. Venkatesan, S. R. Forrest, M. L. Kaplan, C. A. Murray, P. K. Schmidt, and B. J. Wilkens, *J. Appl. Phys.* **54**, 3150 (1983).
- ⁴B. Wasserman, M. S. Dresselhaus, G. Braunstein, G. E. Wnek, and G. Roth, *J. Electron. Mater.* **14**, 157 (1985).
- ⁵B. Wasserman, Ph.D. thesis, Massachusetts Institute of Technology, 1985, p. 99.
- ⁶B. Wassermann, M. S. Dresselhaus, J. D. Woodhouse, M. Wolf, and G. Wnek, *J. Appl. Phys.* (to be published).
- ⁷H. E. Stanley, *J. Stat. Phys.* **36**, 843 (1984).
- ⁸G. E. Wnek, B. Wasserman, M. S. Dresselhaus, S. E. Tunney, and J. K. Stille, *J. Polym. Sci. Polym. Lett. Ed.* **23**, 609 (1985).
- ⁹B. A. Khan and D. Adler (unpublished).
- ¹⁰J. L. Lindhard, M. Scharff, and H. E. Schiott, *Mat. Fys. Medd. Dan. Vid. Selsk.* **33**, 14 (1963).
- ¹¹B. S. Elman, M. K. Thakur, and R. J. Seymour (unpublished).
- ¹²T. Venkatesan, W. L. Brown, C. A. Murray, K. J. Marcantonio, and B. J. Wilkens, *Polym. Eng. Sci.* **23**, 931 (1983).
- ¹³S. Havlin, Z. V. Djordjevic, I. Majid, H. E. Stanley, and G. H. Weiss, *Phys. Rev. Lett.* **53**, 178 (1984).
- ¹⁴P. Meakin, H. E. Stanley, A. Coniglio, and T. A. Witten, *Phys. Rev. A* **32** (1985).
- ¹⁵A. J. Lovinger, S. R. Forrest, M. L. Kaplan, P. H. Schmidt, T. Venkatesan, *J. Appl. Phys.* **55**, 476 (1984).
- ¹⁶M. F. Schlesinger and E. W. Montroll, *Proc. Nat. Acad. Sci. U.S.A.* **81**, 1280 (1984).
- ¹⁷J. D. Carlson, J. E. Bares, A. M. Guzman, and P. P. Pronko, *Nucl. Instrum. Methods Phys. Res.* **B7/8**, 507 (1985).